

dynamics flow is believed to be one major source of the corona instabilities.^{5,6}

¹L. Civitano, G. Dinelli, F. Busi, M. D'Angelantonio, I. Gallimberti, and M. Rea, "Flue Gas Simultaneous DeNO_x/DeSO_x by Impulse Corona Energization," International Atomic Energy Agency, Report No. TECDC-428, pp. 55-84, 1987 (unpublished).

²M. Horvath, *Ozone* (Elsevier, Amsterdam, 1980).

³Electrostatic Society of Japan, in *Electrostatics Hand Book*, Ch. 15 edited by S. Masuda (Ohm, Tokyo, 1984), Chap. 15.

⁴T. Yamamoto and H. R. Velkoff, *J. Fluid Mech.* **108**, 1 (1981).

⁵A. Yabe, Y. Mori, and K. Hijikata, *Am. Inst. Aeronaut. Astronaut. J.* **16**, 340 (1978).

⁶P. Atten, F. M. J. McCluskey, and A. C. Lajomri, *IEEE Trans. Ind. Appl. IA23*, 705 (1987).

Selectively δ -doped quantum well transistor grown by gas-source molecular-beam epitaxy

T. Y. Kuo, J. E. Cunningham, E. F. Schubert, W. T. Tsang, and T. H. Chiu
AT&T Bell Laboratories, Holmdel, New Jersey 07733

F. Ren
AT&T Bell Laboratories, Murray Hill, New Jersey 07974

C. G. Fonstad
Massachusetts Institute of Technology, Cambridge, Massachusetts 02139

(Received 17 December 1987; accepted for publication 27 May 1988)

We report electrical measurements on structures generated by δ doping the AlGaAs barriers of a GaAs quantum well. These structures are made unique by quantum size effects that occur both in the δ -doped barrier and in the GaAs well. Both the Hall-effect and capacitance-voltage measurements reveal that high-density, $4 \times 10^{12} \text{ cm}^{-2}$, two-dimensional electron gas forms in the well along with good mobility. We fabricate field-effect transistors with this structure to obtain transconductances of 300 mS/mm.

The principle of selective doping in semiconductors was introduced nearly 10 years ago by Störmer and Dingle.¹ The principle allows carriers to be spatially separated from parent donors so that high two-dimensional electron gas (2DEG) mobility can be achieved. Technologically important devices in the form of field-effect transistors (FETs) have also employed the concept owing to the high channel conductivity achievable.² These devices have also been the subject of both technical and historical review.^{3,4} It is one further property of this principle when applied in the AlGaAs system that the 2DEG density $n_{2\text{DEG}}$ is confined by fundamental limitations to take values below $1 \times 10^{12} \text{ cm}^{-2}$. Such a limitation arises in the AlGaAs system mainly from the occurrence of both a finite conduction-band discontinuity and solubility limit in concentration of the impurity doping. Recently, it has become possible to overcome $n_{2\text{DEG}}$ limitations by δ doping the barrier of an AlGaAs/GaAs heterostructure.⁵ In comparison to SDH structures using homogeneous doping, $n_{2\text{DEG}}$ values can be enhanced by nearly a factor of 2, an effect that has further been attributed to the quantum size effect that occurs in the δ -doped barrier.⁵

The extension of the selectively δ doping principle to quantum wells in AlGaAs system has previously been reported by Chen *et al.*⁶ Here we evaluate 2DEG formation in the well of structures also employing the selective δ doping concept. We report the Hall-effect and capacitance-voltage (C - V) measurements which show that very high $n_{2\text{DEG}}$ are achievable along with favorable mobility enhancements. When such structures are fabricated into transistors, high

transconductances of 300 mS/mm have been obtained for the first time.

The quantum well structures reported here are grown with gas-source molecular-beam epitaxy methods on undoped (100)-oriented GaAs substrates. In our growth approach elemental solid sources are used for both doping and group-III species while thermally decomposed arsine provides the group-V flux. A schematic of layer sequences associated with this structure is shown in Fig. 1(a). The δ -doped components were achieved via growth interruption prior to the deposition of a fractional Si monolayer coverage under arsenic stabilized surface conditions. An asymmetry in concentration of the δ doping on either side of the well was chosen to compensate in part for the presence of surface states which are known to deplete mobile 2D carriers. To achieve high electron concentrations in the well, short spacer thicknesses were employed and ranged from 15 to 70 Å.

In the δ doping concept,⁷ Si atoms replace some group-III sites in one sublattice plane thereby generating a V-shaped potential of sufficient strength to quantize carriers into energy eigenstates. For increasing Si areal concentrations, the depth of the V-shaped potential increases along with a corresponding increase in size quantization of the carriers. An approximate conduction-band diagram formed by the structure of Fig. 1(a) is shown in Fig. 1(b) with E_F , the Fermi energy, and E_0 , E'_0 the lowest eigenstate energies of the well and δ -doped barriers, respectively. Based on the parameters used in the structure shown in Fig. 1(a), we estimate E'_0 and E_0 to be 120 and 35 meV, respectively. Accord-

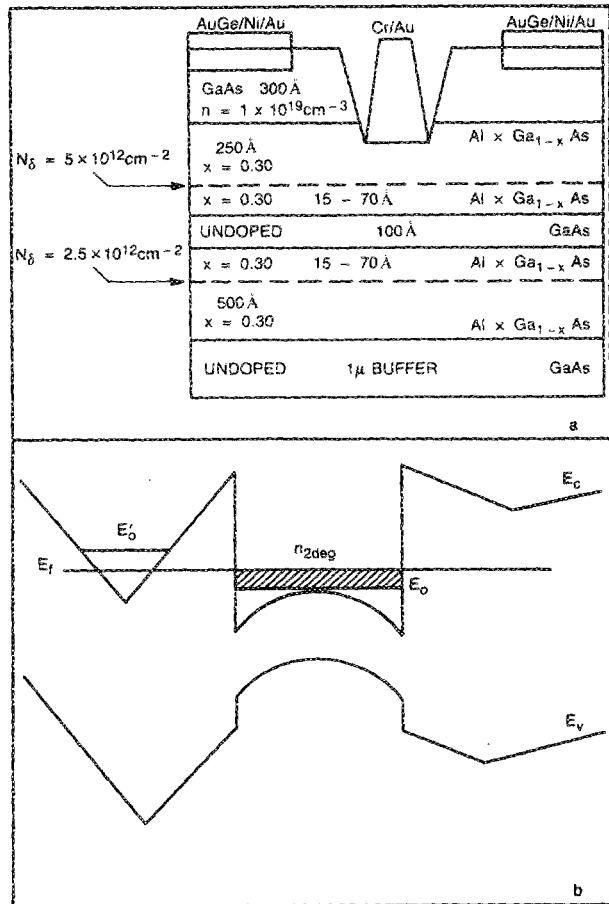


FIG. 1(a): Layer sequence and parameters employed in a selectively δ -doped quantum well. 1(b): The corresponding hypothetical conduction- and valence-band diagram for an equilibrated structure.

ing to Fig. 1(b) parallel transport in the AlGaAs layer can occur when E_f exceeds E'_0 . It is now known *a priori* that E'_0 of the δ -doped barrier lies above the Fermi energy as is depicted in Fig. 1(b). However, approximate model calculations⁵ of the transfer energetics for electrons in this particular structure do confirm this assignment.

Several advantages in 2DEG formation are expected from the use of δ doping when compared to those cases employing homogeneously doped barriers. In structures have a homogeneously doped barrier, the Fermi level lies close to the conduction-band bottom of the AlGaAs for typical doping densities ($1 \times 10^{18} \text{ cm}^{-3}$). Thus for the present δ -doped quantum well structures, when compared to structures differing only by the use of homogeneous doping, we expect that larger $n_{2\text{DEG}}$ forms in the well because E'_0 is upshifted above the AlGaAs conduction-band bottom by quantum size effects. Furthermore, reduced parallel conduction from the δ -doped barriers is expected because E'_0 lies above E_f . Another possible consequence of technical importance introduced by these new δ -doped quantum well structures is that pregrowth interruption is necessarily employed in close proximity to quantum well formation. By analogy to other forms of pregrowth interruption involving either growth stops⁸ or short-period superlattices,⁹ the quality of quantum wells can be expected to be significantly improved. The width of the quantum well L_z plays an important role in

optimizing low field conductivity (mobility \times density) in these structures. In particular, eigenstate energy upshifts should be large (small L_z) in order to suppress both remote ionized impurity scattering and interfacial roughness scattering. This follows from the fact that each scattering process is known to be reduced for increasing kinetic energy of carriers. However, too large an eigenstate energy upshift is not favorable for high electron density formation in the well. In addition, for L_z exceeding 130 Å, a bimodal wave function forms in the well¹⁰ which gives the structure characteristics resembling carrier confinement by a heterointerface potential. As a preliminary step in these investigations, we study structures in which L_z was ~ 100 Å, a choice roughly compromising the above considerations.

The field-effect transistor configuration that was applied to these structures used a standard three-step photolithography method, with active mesa definition constituting the first step. AuGe/Ni/Au metalization of the source-drain electrodes was alloyed for 30 s at 410 °C to facilitate ohmic contact formations. Specific contact resistance of 0.5 $\Omega \text{ mm}$ could be achieved when the structures were terminated with n^+ GaAs layers 300 Å thick and doped to $1 \times 10^{19} \text{ cm}^{-3}$. Recess etching followed by Ti-Au (500 Å/1000 Å) metalization was then employed for the Schottky gate contact.

Both the Hall-effect and C - V measurements were performed on structures grown without a heavily doped cap layer in order to evaluate $n_{2\text{DEG}}$ formation. Room-temperature Hall effect gave a mobility of 3200 $\text{cm}^2/\text{V s}$ and sheet carrier concentration of $4 \times 10^{12} \text{ cm}^{-2}$. The $n_{2\text{DEG}}$ found here is among the highest values reported for a quantum well in the AlGaAs system. Furthermore, the mobility of quantum well carriers is enhanced when compared to the case of GaAs homogeneously doped to an equivalent three-dimensional concentration of $8 \times 10^{18} \text{ cm}^{-3}$. Based on the empirical relationship established by Hilsum, mobilities of 1100 $\text{cm}^2/\text{V s}$ are expected at these three-dimensional densities.¹¹ The quantum well mobility increases to 18 300 $\text{cm}^2/\text{V s}$ at 77 K with a $n_{2\text{DEG}}$ of $3.2 \times 10^{12} \text{ cm}^{-2}$. Clearly good 2D confinement of carriers is indicated by the Hall effect.

We have also performed C - V measurements on this same device structure using mercury probe contacts. C - V profiling is used to spatially resolve carrier distributions in semiconductors. In quantum-mechanical systems such as heterostructures and quantum wells, the C - V profile does not necessarily coincide with the free carrier concentration, nor the doping profile. Instead, the C - V profile can reflect the response of wave-function centroid under the external bias perturbation.¹² The centroid of a wave function in a quantum well will, however, always be localized within the well even under external bias. Therefore, we expect the width of the C - V profile to be narrower or equal to the width of the quantum well.

The C - V profile of a GaAs quantum well is shown in Fig. 2. A peak is observed at a normalized C - V distance of 300 Å, which coincides with the distance of the well center below the Schottky contact. We observe a C - V profile width of 120 Å which is comparable to the width of the quantum well (90 Å). In addition the area under the C - V peak corre-

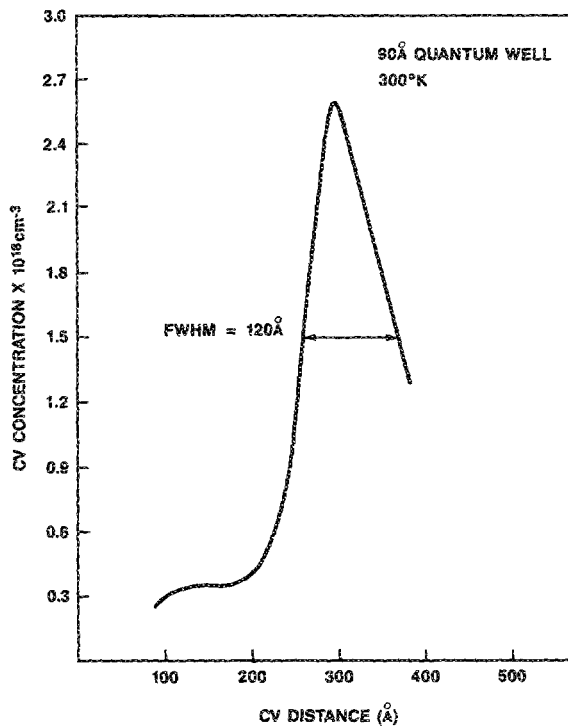
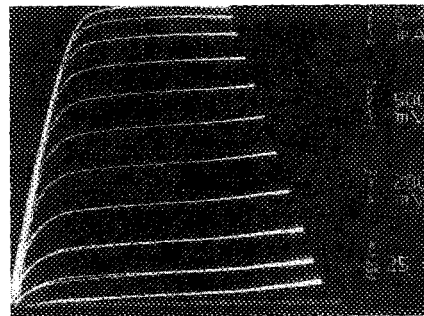


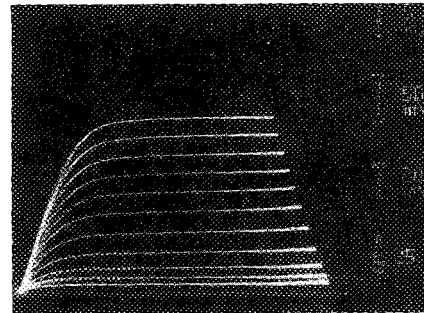
FIG. 2. Capacitance-voltage measurement of a selectively δ -doped 90 Å quantum well.

sponds to a density of $3.8 \times 10^{12} \text{ cm}^{-2}$, a result in agreement with the carrier concentration derived from the Hall effect. Furthermore, we observe no other profile components on the wings of the C - V response. The latter observation also implies carriers reside in the quantum well and not in the δ -doped barriers based on the following consideration. In 3D systems, spatial changes in the doping profile cannot be well resolved over distances shorter than the Debye length. In 2D systems such as the δ -doped structure, the resolvable spatial length corresponds to the spatial extent of the 2D wave function. The spatial extent of the 2D wave function in the δ -doped barrier, if occupied by carriers, is 60 Å.¹² The δ -doping planes are separated from the well center by 120 Å and spatial resolution of a two-carrier profile remains possible.

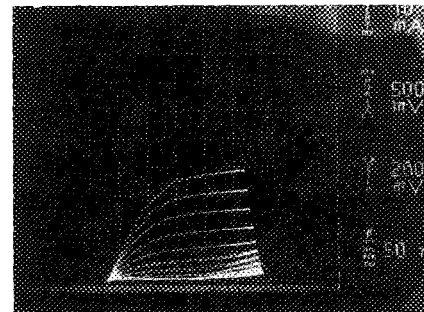
The current-voltage output characteristics of FET configurations applied to this same 90 Å quantum well structure are shown in Figs. 3(a) and 3(b) and correspond to gate length of 2.2 and 1.2 μm , respectively. All gate widths for all devices were 150 μm . Excellent on-resistances are indicated by both Figs. 3(a) and 3(b) with good saturation and pinch-off voltage behavior. The transconductances deduced from Fig. 3(b) is 260 mS/mm. One factor limiting the transconductances of Figs. 3(a) and 3(b) is the absence of a heavily doped cap layer to assist ohmic contact formation. The current-voltage output characteristics of an improved structure employing the heavily doped cap layer discussed earlier as well as shortening spacer thickness to 15 Å is presented in Fig. 3(c). The corresponding transconductance is 300 mS/mm for a transistor gate length of 1.2 μm . In addition, both Figs. 3(a) and 3(c) demonstrate further that very large $n_{2\text{DEG}}$ provided by these quantum well structures can be fully depleted.



a



b



c

FIG. 3. Current-voltage output characteristics for several selectively δ -doped quantum well transistors. Details of the structure corresponding to each trace are found in the text.

In summary we have investigated a new structure formed by δ doping the barriers of a GaAs quantum well. Hall measurements reveal that high $n_{2\text{DEG}}$ are achievable along with favorable mobility enhancements. Capacitance-voltage characteristics confirm efficient carrier transfer to the quantum well. Very high transconductances of 300 mS/mm have also been realized in these structures employing an FET configuration.

T. Y. Kuo would like to thank the Hertz Foundation for support.

¹R. Dingle, H. L. Störmer, A. C. Gossard, and W. Wiegmann, *Appl. Phys. Lett.* **33**, 665 (1978).

²T. Mimura, T. K. Joskin, S. Hiyamizu, K. Hikosaka, and M. Abe, *Jpn. J. Appl. Phys.* **20**, L598 (1981).

³P. Solomon and H. Morkoç, *IEEE Trans. on Electron. Device* **ED-31**, 1015 (1984).

⁴R. Dingle, M. D. Feuer, and C. W. Tu, in *VLSI Electronics*, edited by N.

G. Einspruch and W. R. Weisman, (Academic, New York, 1985), p. 216.
³J. E. Cunningham, W. T. Tsang, G. Timp, E. F. Schubert, A. M. Chang, and K. Owusu-Sekyere, *Phys. Rev. B* **37**, 4317 (1988).
⁴Y. K. Chen, D. C. Radulescu, P. J. Tasker, G. W. Wang, and L. F. Eastman, *GaAs and Related Compounds*, edited by W. T. Lindley (The Institute of Physics, Bristol, England, 1987), p. 581.
⁵C. E. C. Wood, G. Metzger, J. Berry, and L. F. Eastman, *J. Appl. Phys.* **51**, 383 (1980).

⁸H. Sakaki, M. Tanka, and J. Yoshino, *Jpn. J. Appl. Phys.* **24**, L417 (1985).

⁹G. Weiman and W. Schlapp, *Appl. Phys. A* **37**, 139 (1985).

¹⁰S. Sasa, J. Saito, D. Nanbu, T. Ishikawa, and S. M. Inoue, *Jpn. J. Appl. Phys.* **24**, L281 (1985).

¹¹C. Hilsum, *Electron. Lett.* **10**, 259 (1974).

¹²E. F. Schubert, J. B. Stark, B. Ullrich, and J. E. Cunningham, *Appl. Phys. Lett.* **52**, 1510 (1988).

Optical properties at the metal-insulator transition in thermochromic $\text{VO}_{2-x}\text{F}_x$ thin films

K. A. Khan,^{a)} G. A. Niklasson, and C. G. Granqvist

Physics Department, Chalmers University of Technology, S-412 96 Gothenburg, Sweden

(Received 10 May 1988; accepted for publication 2 June 1988)

Thermochromic $\text{VO}_{2-x}\text{F}_x$ thin films were prepared by reactive rf magnetron sputtering followed by annealing post-treatment. Electrical and optical properties were measured as a function of temperature. The transmittance and reflectance were essentially wavelength independent at 65 °C, i.e., at the metal-insulator transition.

This communication reports on temperature-dependent optical properties of thin VO_2 -based films. The transmittance is found to be spectrally independent at a temperature which corresponds to a metal-insulator transition (MIT).

MITs have been studied for many materials and by many techniques.¹ Recently it has been found from optical measurements that the spectral transmittance and reflectance become essentially wavelength independent at the MIT, which takes place at a certain "critical" thickness in extremely thin films of Au (Refs. 2–5) and Al (Refs. 2 and 6). Scaling arguments have been put forward³ to theoretically account for the data, but no detailed understanding has been reached. It has been stated⁵—although no data have yet been reported—that spectral independence occurs also in metal-insulator composites having a "critical" metal fraction corresponding to a MIT. It is of considerable interest to see whether an analogous simple "fingerprint" of the MIT can be applied to other types of materials. It will be shown below that spectrally independent optical properties indeed are found at the MIT in (0.1–0.2)- μm -thick thermochromic vanadium oxyfluoride films.

Several vanadium oxides exhibit MITs.^{1,7–9} The one in VO_2 is of particular interest since it occurs at a temperature τ_c of ~ 68 °C (in bulk material), i.e., in a convenient range for experiments. The low-temperature phase is monoclinic with V–V separations alternating between two different values and V–V pairs tilted slightly off the monoclinic a axis.⁸ The high-temperature phase is tetragonal and is characterized by chains of equidistant V atoms along the c axis. The MIT has been described theoretically as a Mott–Hubbard-type transition^{1,7} (caused, essentially, by the off-axis displacement of the V atoms), or by electron trapping in homopolar bonds^{8,9} (associated with the pairing of the V atoms). Recent work¹⁰ has given support to the latter view. The MIT

occurs within a very narrow temperature range for single crystals of VO_2 . In thin films, however, the transition can be smeared over several °C. Optical data for thin films have been interpreted^{11–14} on the premise that the material forms a percolation structure comprising metallic and insulating parts. The evidence is based on anomalous absorption¹¹ and transition opalescence¹³ at τ_c as well as on critical exponents¹² for the MIT evaluated from conductivity measurements. It is possible to diminish τ_c by several techniques¹⁵ including a substitution of V^{4+} by penta- or hexavalent ions or by replacing some of the oxygen by fluorine.^{16–18} In the present work we study $\text{VO}_{2-x}\text{F}_x$ with $\tau_c \sim 52$ °C; the lowering of τ_c facilitates an accurate optical analysis in the temperature region around the MIT.

Thermochromic $\text{VO}_{2-x}\text{F}_x$ thin films were produced by reactive rf-magnetron sputtering followed by annealing post-treatment. Sputtering was conducted in the unit described in Ref. 19. After evacuation to $< 1.5 \times 10^{-6}$ Torr by cryopumping, a mixture of Ar (purity 99.9997%), O_2 (purity 99.998%), and CF_4 (purity 99.995%) was introduced to a total pressure 7.6×10^{-3} Torr. The gas composition was maintained by letting in the constituents via flow controlled regulators at the rates 28 scc/min for Ar, 0.7 scc/min for O_2 , and 1.0 scc/min for CF_4 , where scc denotes standard cubic centimeter. Sputtering took place from a 10-cm-diam planar vanadium target (purity 99.8%) onto substrates of Corning 7059 glass and of Be foil positioned 4.5 cm below the target surface. The discharge power was 200 W at 13.56 MHz. The substrates were fastened to a radiatively heated surface whose temperature remained at 400 to 450 °C, as determined by a Chromel–Alumel thermocouple. Presputtering was conducted for about 20 min before the actual thin-film deposition began. The annealing post-treatment was performed in 1.2 Torr of air during 2 h in a vacuum oven heated to 420 °C. Thickness determinations on annealed films, using a Tencor Alpha-Step instrument, yielded an effective thin-film growth rate of 0.22 nm s^{-1} .

^{a)} Permanent address: Dept. of Applied Physics and Electronics, Rajshahi University, Rajshahi, Bangladesh.